

## Effect of pion thermal width on the sigma spectrum

Yoshimasa HIDA KATA, O사무 M ORIMATSU, Tetsuo NISHIKAWA, and Munehisa OHTANI<sup>1\*</sup>  
 Institute of Particle and Nuclear Studies, High Energy Accelerator  
 Research Organization, 1-1, Oho, Tsuruga, Ibaraki, 305-0801, Japan  
 (Dated: May 22, 2019)

We study the effect of thermal width of  $\pi$  on the spectral function of  $\sigma$  applying a resummation technique called optimized perturbation theory at finite temperature ( $T$ ) to  $O(4)$  linear sigma model. In order to take into account finite thermal width of  $\pi$ , we replace the internal pion mass in the self-energy of  $\pi$  with that of complex pole found in a previous paper. The obtained spectral function for  $T > 100$  MeV turns out to possess two broad peaks. The sharp peak at  $T = 0$  threshold is smeared out, which was observed in the one-loop calculation without pion thermal width. We also search for the poles of the propagator, which is helpful for deeper understanding the behavior of the spectral function.

PACS numbers: 11.10.Wx, 12.40.-y, 14.40.Aq, 14.40.Cs, 25.75.-q

Keywords: sigma meson, pion, spectral function, finite temperature, thermal width, linear sigma model

It is now believed that chiral symmetry is restored at high temperature. This implies that the mass of  $\sigma$  decreases while that of  $\pi$  increases with increasing temperature. At certain temperature, therefore, the mass of  $\sigma$  coincides with twice that of  $\pi$ . Accordingly, the spectrum of  $\sigma$  is expected to be enhanced near the threshold of  $T = 0$ , since the phase space available for the decay is squeezed to zero.

Chiku and Hatsuwa [1] showed that the threshold enhancement in the  $\sigma\pi\pi$  channel is observed as expected. According to their analysis,  $\sigma$  has also finite width which comes from the induced decay by the scattering with thermal pions in the heat bath:  $\sigma \rightarrow \pi\pi$  thermal !. The width of  $\sigma$  is 50 MeV at the temperature where the threshold in the spectrum is most strongly enhanced. In their analysis of the spectrum of  $\sigma$ , however, the effect of the pion thermal width is not included, since they calculated the self-energy only up to one-loop order. The purpose of this paper is to show that the threshold enhancement is smeared out by taking into account the effect of pion thermal width.

Our strategy is as follows. We use the one-loop self-energy for  $\sigma$ , but we replace the masses of internal pions with complex ones. This complex mass was obtained from the location of the pole of the pion propagator in a previous work [2]. Using the self-energy with the complex pion mass, we reanalyze the spectral function of  $\sigma$ . The poles of the propagator are also searched for to understand the behavior of the spectral function.

Along the lines mentioned above, we employ the  $O(4)$  linear sigma model:

$$L = \frac{1}{2}(\partial_\mu\phi)^2 - \frac{1}{2}m^2\phi^2 - \frac{1}{4!}(\partial_\mu\phi)^2 + h\phi; \quad (1)$$

with  $\phi = (\phi_0; \phi_1)$ . As the chiral symmetry is taken to be dynamically broken at low  $T$ , the quadratic term in the Lagrangian has negative sign,  $m^2 < 0$ . Owing to this choice of the sign and the explicit breaking term of  $h\phi_0$ , the field  $\phi_0$  has a non-vanishing expectation value  $\langle\phi_0\rangle$ . In

this prospect, we decompose beforehand the field operator  $\phi_0$  into the classical condensate and the quantum fluctuation as  $\phi_0 = \langle\phi_0\rangle + \phi_1$ .

Integrating out the quadratic of the fluctuations and around the condensate, we obtain the one-loop effective potential  $V^e(T)$ . As a minimum of the effective potential, the condensate  $\langle\phi_0\rangle(T)$  is determined and this leads us to the gap equation,

$$0 = \frac{\partial V^e}{\partial \langle\phi_0\rangle} = h + \frac{m^2}{3!} + \frac{1}{2}(\Gamma^{(1)} + \Gamma^{(1)}): \quad (2)$$

The model parameters are fixed so as to reproduce the experimental values of the pion mass ( $m_0$ ), the pion decay constant ( $F_0$ ) and the peak energy of the spectral function  $\sigma$  at  $T = 0$  following Ref.[1]:  $m_0^2 = (283\text{ MeV})^2$ ;  $F_0 = 73.0$ ;  $h = (123\text{ MeV})^3$ . The last term in eq. (2) is contribution from the tadpole diagrams in the modified minimal subtraction scheme (MS):

$$\Gamma^{(1)} \equiv \frac{m_0^2}{16\pi^2} \left( 1 - \ln \frac{m_0^2}{2} \right) + \frac{Z_1}{2} \frac{dp^2}{2^2} \frac{n(!)}{!}; \quad (3)$$

with  $\frac{dp}{!} = \frac{1}{p^2 + m_0^2}$  and  $n(!) = (e^{1/T} - 1)^{-1}$ .  $Z_1$  is the renormalization point.  $m_0$  and  $m_0$  are the tree-level masses of the fluctuations defined by

$$m_0^2 = m^2 + \frac{2}{2}; \quad m_0^2 = m^2 + \frac{2}{6};$$

where  $m(T)$  is an optimal mass parameter introduced in the framework of the optimized perturbation theory (OPT) [1, 3].

A physical concept of OPT is to impose thermal effects upon the optimal parameter(s) and to tune it by an optimal condition [3]. In our case,  $m$  is determined so that the (thermal part of) pion mass correction vanishes at zero momentum [1].

Making use of the OPT, the threshold enhancement of the spectral function of  $\sigma$  was reported [1]. In order to understand how this enhancement occurs and will

be smeared by the thermal width of  $\pi$ , it is important to consider the scattering with thermal pions as mentioned previously. At the same time, it is also of much account to clarify analyticity of the self-energy as well. This is basically because the spectral function, which is the imaginary part of the propagator, is related to the self-energy  $(k; T)$  as

$$\begin{aligned} (k; T) &= 2 \operatorname{Im} D(k; T) \\ &= 2 \operatorname{Im} (k^2 - m_0^2 - (k; T))^1; \end{aligned} \quad (4)$$

with  $k = (0; k)$ . At one-loop level, the self-energy is written as

$$(k; T) = \frac{(m^2 - k^2)^2}{2^2} + \frac{1}{2} I^{(1)} + I^{(1)} - \frac{1}{2} I^{(2)} + \frac{1}{3} I^{(2)}; \quad (5)$$

where  $I^{(2)}$  corresponds to a bubble diagram shown in Fig.1,

$$\begin{aligned} I^{(2)} &\stackrel{\text{MS}}{=} \frac{1}{16} \int_0^{\infty} \frac{2}{\pi} \ln \frac{m_0^2}{p^2} + c \ln \frac{c}{c+1} \\ &\quad - \frac{1}{2} \int_0^{\infty} \frac{Z}{p^2} \frac{dp}{p} \frac{p^2}{k^2} \frac{n(\pi)}{4\pi^2}; \end{aligned} \quad (6)$$

$$\text{with } c = \frac{q}{1 - 4m_0^2/k^2}.$$

Now, we are ready to consider effects of pion thermal width on the spectrum of  $\pi$ . Although the width can be estimated directly from relevant scattering processes, we adopt more simple prescription [1] to use a complex pion pole as internal pion mass in (5). The thermal width of  $\pi$  is represented in the imaginary part of the complex pole of the pion propagator:

$$\begin{aligned} D^{-1} &= p^2 - m_0^2 - (p^2; p; T)_{p^2 = (m^{\text{pole}})^2} = 0; \\ m^{\text{pole}} &= m(T) - i \frac{T}{2}; \end{aligned}$$

where  $(p^2; p; T)$  is the pion self-energy.

As a matter of course, the pole has dependence of  $p^2$  naturally [2], but contributions from  $p^2$  &  $T$  are less effective to the loop integration in the thermal part of  $\pi$ . Therefore, as a simple recipe to incorporate the thermal width, we replace  $m_0$  in Eq.(5) with  $m^{\text{pole}}$  at  $p = 0$  in Ref.[2] as depicted in Fig.1 and substitute it into Eq.(4) to obtain  $\pi$ .

We show in Fig.2 the obtained spectral function, Eq.(4), at  $k = 0$  for several values of  $T$ . For comparison, we also show the spectral function at  $T = 145$  MeV with  $m_0$  and that with  $m^{\text{pole}}$  in Fig.3. At low  $T$  the spectrum consists of a broad bump around  $\omega = 550$  MeV. As  $T$  increases, another strength grows at the left shoulder of the bump, while the spectrum for  $\omega > 400$  MeV does not vary much. In contrast to this case, if  $m_0$  is

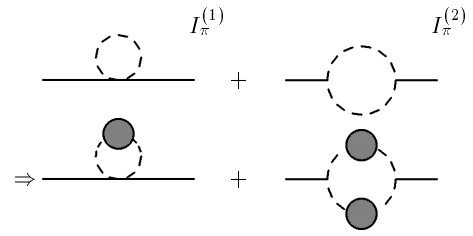


FIG.1: A prescription to take into account the thermal width of  $\pi$  in the decay  $\pi \rightarrow \pi$ . The upper diagrams represent the self-energy of  $\pi$ , Eqs.(3) and (6), with the internal pion mass,  $m_0$ , and the lower diagrams with  $m^{\text{pole}}$ .

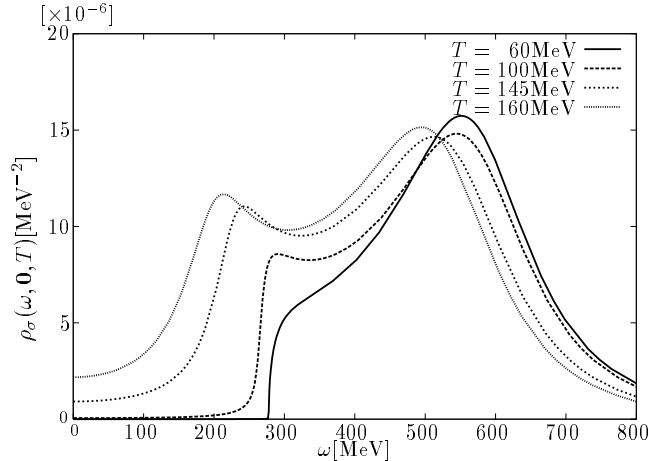


FIG.2: Spectral function of  $\pi$ , Eq.(4), with the thermal width of  $\pi$ .

used as the internal pion mass, the spectrum near the threshold of  $\pi$  is enhanced as  $T$  is increased. At  $T = 145$  MeV, where the mass of  $\pi$  coincides with  $2m_0$ , the spectrum near the threshold is most strongly enhanced as shown in Fig.3 (dotted curve). When  $m^{\text{pole}}$  is used, however, due to the thermal width of  $\pi$  in the decay  $\pi \rightarrow \pi$ , the sharp threshold is smeared to be a bump at  $\omega = 200$  MeV – 300 MeV as the solid curve in Fig.3.

In general, the behavior of spectral function is governed by poles of the propagator. We thus next search for the poles of propagator on the complex  $\omega$  plane. As can be clearly seen from Eq.(4) the analytic structure of the propagator is determined by that of the self-energy. Then, from Eq.(5) and Eq.(6) we see that the self-energy has a branch point at  $\omega = 2m^{\text{pole}}$  around which the Riemann sheet is two-fold. The self-energy has another branch point due to loop which, however, is irrelevant for the present discussion of the self-energy around the threshold of  $\pi$ . The branch cut from  $\omega = 2m^{\text{pole}}$  can be arbitrarily chosen at finite temperature, because it has no physical meaning. For definiteness we choose

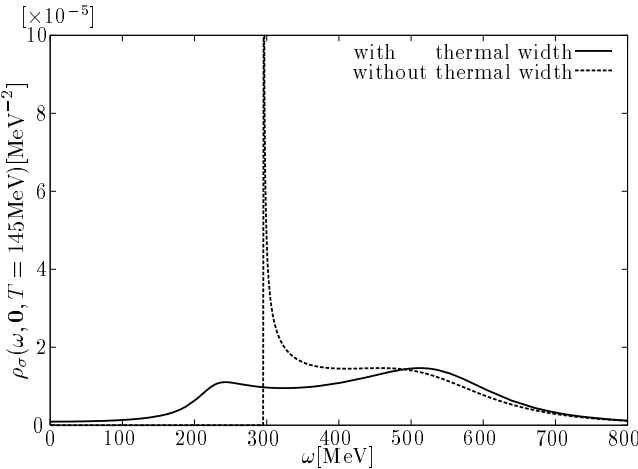


FIG. 3: Spectral function of with and without the thermal width of at  $T = 145$  MeV.

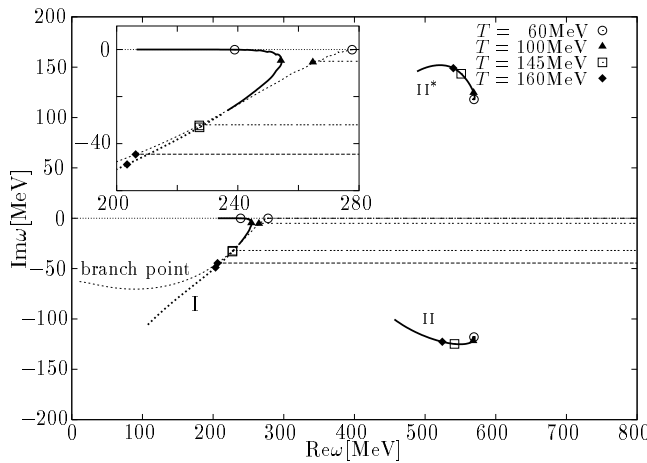


FIG. 4: Location of the poles of the propagator with the thermal width of,  $m_pole$ . The branch point is shown by dotted line and the branch cut are also indicated.

the cut from the branch point straight to the right, parallel to the real axis and refer to the sheet including the physical real energy as the first Riemann sheet and the other one as the second Riemann sheet. We show in Fig.4 the result of searching the locations of the poles on the Riemann sheets.

We found three relevant poles. Two of them, (II) and (II\*), are on the second Riemann sheet and on the real axis. Their positions are approximately symmetric with respect to the real axis with each other. For the spectral function of, on one hand, (II) and (II\*) show up as a bump around  $\omega = 550$  MeV and the small movement of these poles explains the insensitivity to  $T$  of the spectrum for  $\omega \approx 400$  MeV. On the other hand, the structure of the spectrum for low  $\omega$  is mainly determined by the remaining one pole, (I). For preparation to consider this pole

(I), let us first recall the movement of the corresponding pole in case of no thermal width of [2].

Without the pion width, the counterpart of the pole (I) exists on the second Riemann sheet apart from the branch point of  $2m_0$  for  $T = 60$  MeV. Correspondingly, the spectrum has no peak at the threshold for low  $T$ . As  $T$  increases, the pole moves along the real axis from below toward the branch point  $2m_0$  and turns around at the point to appear on the first sheet at  $T = 145$  MeV. In response to this movement, the spectrum is strongly enhanced for  $T = 145$  MeV. In other words, the threshold enhancement originates in the fact that the pole approaches the branch point on the real axis near the temperature concerned.

Keeping this in mind, we return to the discussion on movement of the pole (I) next. As is the case with no pion width, this pole also resides on the second Riemann sheet for low  $T$  and comes closer to the branch point with increasing  $T$  as shown in Fig. 4. At  $T = 138$  MeV, the pole crosses the branch cut and appears on the first Riemann sheet from the second, likewise. The branch point, however, is located at  $2m_pole$  apart from the real axis for  $T = 100$  MeV due to the finite thermal width of (see Fig. 4). The complex branch point demands that the pole (I), whose counterpart caused the threshold enhancement by moving toward the point, also acquires an imaginary part near  $T = 138$  MeV. As a result, the spectrum is smeared and the remarkable contrast is brought about for the spectrum as shown in Fig. 3.

Let us argue on the correlation between the spectral function and poles of the propagator more quantitatively. For this purpose, we approximate the propagator of with the superposition of the three pole contributions in the following way:

$$Z^{pole} = \frac{1}{2\text{Im}_\text{pole}} \frac{Z_\text{pole}}{q - q_\text{pole}}; \\ Z_\text{pole} = \frac{1}{2q_\text{pole}} \left( 1 - \frac{\partial}{\partial k^2} (k^2 - (m_\text{pole})^2) \right)^{-1}; \quad (7)$$

where  $m_\text{pole}$  stands for the pole of the propagator.  $q$  and  $q_\text{pole}$  are defined by  $q = (k^2 - (2m_\text{pole})^2)^{1/2}$  and  $q_\text{pole} = (m_\text{pole})^2 - (2m_\text{pole})^2)^{1/2}$ , respectively. It should be noted that we have taken not  $k^2$  but  $q = (k^2 - (2m_\text{pole})^2)^{1/2}$  as an appropriate variable. The use of this variable enables us to unfold two leaves of the Riemann sheet around the branch point [4]. We can reflect which Riemann sheet accommodates each pole on the approximated propagator.

We show the approximated spectral function, Eq.(7), for two cases,  $T = 60$  MeV and  $T = 145$  MeV, in Figs.5 and 6, respectively. At  $T = 60$  MeV, pole (I) is located on the second Riemann sheet, while it is on the first sheet at  $T = 145$  MeV. We can see that poles (II) and (II\*) provide the broad peak around  $\omega = 550$  MeV and that pole (I) mainly determine the behavior of the

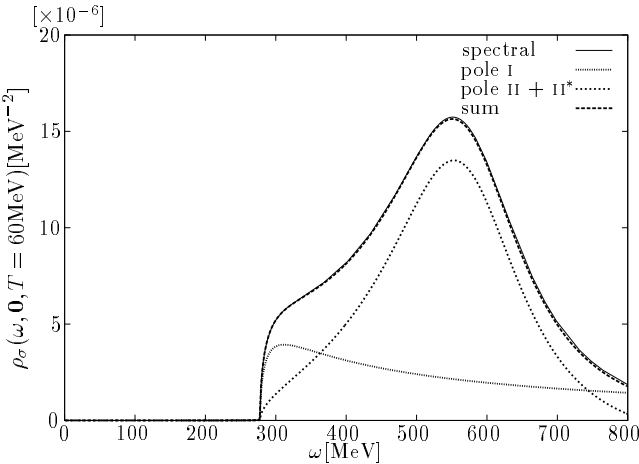


FIG. 5: The spectral function approximated by a superposition of the contributions from the three poles, Eq.(7), at  $T = 60$  MeV. The spectral function, Eq.(4), is also shown.

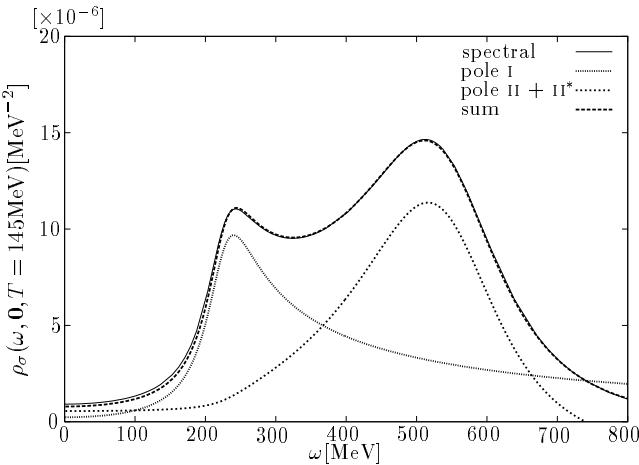


FIG. 6: The same as in Fig.5 at  $T = 145$  MeV.

left shoulder of the peak. If we include only the contributions of (I) and (II), two broad peaks are still reproduced. However, a structure which is not seen in the spectral function appears at low  $\omega$  region. The contribution of (II\*) cancels out the spurious structure caused by (II). At  $T = 60$  MeV, the left shoulder of the peak is small, although pole (I) seems to lie close to the real axis. This is because the pole is on the second Riemann sheet and is practically far from the real axis. In contrast, at  $T = 145$  MeV, pole (I) is on the first Riemann sheet and is close to the real axis. Accordingly, it provides a peak with more strength around  $\omega = 200 - 300$  MeV. Thus, in order to reveal the relation between the poles and the behavior of the spectrum, it is necessary to know both of the complex structure of the Riemann sheet and the positions of the poles on it.

In conclusion, the thermal width of  $\pi$  smears out the

sharp peak of the spectrum at threshold. The structure of the spectral function can be well understood from the three relevant poles of the propagators and the branch points of the self-energy. Physically we can interpret the origin of the smearing as follows. By replacing the masses of  $\pi$  in the decay  $\pi \rightarrow \pi \pi$  with the complex mass, processes like  $\pi \rightarrow \pi \pi$  are newly taken into account. Since this process is allowed for any energy of the initial [5], threshold disappears thereby. Due to the above process, the peak at the threshold is expected to acquire a width of

$$n(E) \propto m^3 \propto 100 \text{ MeV}; \quad (8)$$

where  $E$  is the typical energy of thermal pions.  $n$  is the scattering cross section of  $\pi\pi$  and its value is estimated to be  $O(1/f^2)$  from the low energy theorem. In the present calculation, only the mass shift of the internal pion for the one-loop self-energy is taken into account. One might be worried whether other effects, such as vertex correction and wavefunction renormalization, might drastically change the results. The physical point, however, is that the calculated spectral function using the complex pion mass is consistent with the estimate, Eq.(8). Therefore, the results of the present paper should be essentially correct even after including other effects.

As was discussed in Ref.[1], the behavior of  $n$  is reflected on the diphoton emission rate from the decay  $\pi \rightarrow \gamma\gamma$ . This indicates that the diphoton yield will also be smeared out, which will be reported elsewhere [6]. The smeared behavior of  $n$  is also seen for finite density [7, 8], though physical origin of the width is different. It is interesting to apply the prescription adopted here in the context of finite density system.

What we have observed in this paper is expected to be universal for processes in which a particle decays into unstable particles.

One of the authors (M.O.) would like to thank H. Fujii for fruitful comments and discussions. The authors would like to acknowledge valuable discussions with T. Hatsuda.

---

Electronic address: hidaka@post.kek.jp  
<sup>y</sup> Electronic address: osamu.morimatsu@kek.jp  
<sup>z</sup> Electronic address: nishi@post.kek.jp  
<sup>x</sup> Electronic address: ohtani@post.kek.jp

- [1] S. Chiku and T. Hatsuda, Phys. Rev.D 57, R6 (1998), Phys. Rev.D 58, 76001 (1998)
- [2] Y. Hidaka, O. Morimatsu and T. Nishikawa, Phys. Rev.D 67, 056004 (2003).
- [3] P. M. Stevenson, Phys. Rev.D 23, 1981 (2916).
- [4] R. G. Newton, SCATTERING THEORY OF WAVES AND PARTICLES (New York, USA: Springer, 1982).
- [5] T. Nishikawa, O. Morimatsu and Y. Hidaka, hep-ph/0302098.

- [6] Y. Hidaka, O. Morimatsu, T. Nishikawa and M. Ohtani, in preparation.
- [7] G. Chanfray, nucl-th/0212085.
- [8] F. Bonutti et al, CHAOS Collaboration, Nucl. Phys.A 677, 213 (2000).